Measurement 192 (2022) 110848

Contents lists available at ScienceDirect

Measurement

journal homepage: www.elsevier.com/locate/measurement

Improved line–line method for propagation constant measurement of reflection-asymmetric networks

Ugur Cem Hasar [a,*], Hamdullah Ozturk [a], Huseyin Korkmaz [a], Mucahit Izginli [a,b], Muharrem Karaaslan [c]

[a] Department of Electrical and Electronics Engineering, Gaziantep University, 27310 Gaziantep, Turkey
[b] Department of Electrical and Electronics Engineering, Hasan Kalyoncu University, 27410 Gaziantep, Turkey
[c] Department of Electrical and Electronics Engineering, Iskenderun Technical University, Iskenderun, 31200 Hatay, Turkey

ARTICLE INFO

Keywords:
Line–line method
Reflection-asymmetric network
Propagation constant

ABSTRACT

A new formalism using line–line measurements is proposed to improve the accuracy of propagation constant measurement of reflection-asymmetric networks using non-calibrated scattering (S-) parameters. For this measurement, the method uses a reference network with arbitrary forward and backward impedance, propagation constant, and length, thus giving flexibility in the application of line–line methods. S-parameter measurements were carried out for propagation constant extraction of a reflection-asymmetric waveguide loaded with a bianisotropic metamaterial slab made by C-shaped split-ring-resonators using two different kinds of reference networks (two empty waveguide sections as the first kind and the same sections loaded by polyethylene samples as the second kind). It is observed that the standard deviation in the extracted real part of the propagation constant of this network by our method could be reduced by using the first kind of reference network, indicating that the accuracy of our method could be improved using a suitable reference network.

1. Introduction

Electromagnetic properties of materials or networks can be extracted using various "line-line" (LL) methods through non-calibrated scattering (S-) parameters [1–24]. The general idea behind the LL methods is to extract electromagnetic properties such as propagation constant from measurements of S-parameters of at least two transmission lines differing in lengths only. As examples for transmission lines, coaxial transmission line [1], slotline [7], microstrip line [2], rectangular waveguide [4], and coplanar waveguide [13] can be enumerated. When the available LL methods in the literate are examined, the following points are noted. The method in the studies [2,5,23] uses S-parameter measurements of the two lines with different lengths loaded with the same material, whereas the method in the study [1] utilizes S-parameters of three different positions of the sample within one line. Besides, while the method in the study [16] employs S-parameter measurements of sample-loaded identical lines with different lengths, the method in the studies [10–12,24] applies S-parameter measurements of one sample-loaded line in addition to the thru connection.

All the available LL methods [1–24] are limited to propagation constant determination of lines or electromagnetic properties of samples loaded into lines with symmetric reflections. In a recent study [25], we applied a LL method for propagation constant determination of lines with asymmetric reflections. Such a determination is needed for understanding the propagation characteristics of such lines, such as the tunneling effect in pseudochiral Omega slabs [26] and analysis of pseudoscalar complex chirality and nonreciprocity parameters of omega-type bianisotropic metamaterial (MM) slabs [27]. However, the LL method in the study [25] is just applicable for two lines with the same impedances but different lengths. In this study, a general LL method is proposed for propagation constant measurement of reflection-asymmetric lines/networks incorporating a reference network with arbitrary propagation constant, impedance(s), and length into the theoretical analysis. Such an implementation gives flexibility in evaluating propagation constant measurement of reflection-asymmetric lines/networks using any reference network with known electromagnetic properties (propagation constant and impedance(s)) and physical length. For validation of the proposed method, propagation factor and propagation constant of a reflection asymmetric network, constructed by a bianisotropic MM slabs involving C-shaped split-ring-resonators (SRRs), were measured using average values of uncalibrated S-parameters from ten linearly-independent measurements. Two different kinds of reference networks (the first kind uses two empty

* Corresponding author.
E-mail address: uchasar@gantep.edu.tr (U.C. Hasar).

https://doi.org/10.1016/j.measurement.2022.110848
Received 9 November 2021; Received in revised form 18 January 2022; Accepted 3 February 2022
Available online 19 February 2022
0263-2241/© 2022 Published by Elsevier Ltd.

waveguide sections with different lengths, and the second kind uses the same sections loaded by polyethylene (PE) samples) were used for this goal, as discussed in Section 3. It is noted that measured propagation factor and propagation constant values by our method are, respectively, close to those of the calibration-independent method [25] and those of the calibration-dependent method [27]. Besides, it is also observed that the standard deviations for the real part of the propagation constant determined by our method using the first kind of reference network are, respectively, close to those evaluated from the calibration-independent method [27] and are significantly smaller than those determined from the calibration-independent method [25] and those determined from our method using the second kind reference network. This clearly shows that it is possible to improve the accuracy of propagation constant measurements of reflection-asymmetric networks by our methodology by optimizing propagation constant measurements using different reference networks.

2. The proposed method

The two measurement configurations in application of our method for propagation constant determination of a reflection-asymmetric network are shown in Figs. 1(a) and 1(b). Fig. 1(a) illustrates the measurement configuration where a reflection-asymmetric two-port network with the forward and backward wave impedances Z_{w1}^{+} and Z_{w1}^{-}, the propagation constant γ_1, and the length l_1 is connected between two two-port error networks X and Y. Here, the networks X and Y represent imperfections of a vector network analyzer (VNA) (frequency error, source and load match error, etc.) and transition errors and phase changes between the output of the VNA and the reflection-asymmetric (and reference) network. On the other hand, Fig. 1(b) illustrates the measurement configuration where a reference two-port network with known forward and backward wave impedances Z_{w2}^{+} and Z_{w2}^{-}, propagation constant γ_2, and length l_2 is connected between the same X and Y networks.

The total wave-cascading matrices (WCMs) of the measurement configurations in Figs. 1(a) and 1(b) can be written as

$$M_1 = T_X \cdot R_1^{Z_0,Z_0}(l_1) \cdot T_Y, \tag{1}$$

$$M_2 = T_X \cdot R_2^{Z_0,Z_0}(l_2) \cdot T_Y, \tag{2}$$

where $R_1^{Z_0,Z_0}(l_1)$ and $R_2^{Z_0,Z_0}(l_2)$ denote the WCMs of the reflection-asymmetric network and the reference network both of which are referenced to the same characteristic impedance Z_0 whose value can be different than Z_{w2}^{+} and Z_{w2}^{-}; and T_X and T_Y represent the WCMs of the two-port networks X and Y, respectively.

The WCMs $R_1^{Z_0,Z_0}(l_1)$ and $R_2^{Z_0,Z_0}(l_2)$ can be separated into three parts [25] as

$$R_1^{Z_0,Z_0}(l_1) = Q^{Z_0,Z_{w1}^{\mp}} \cdot R^{Z_{w1}^{\mp},Z_{w1}^{\mp}} \cdot Q^{Z_{w1}^{\mp},Z_0} \tag{3}$$

$$R_2^{Z_0,Z_0}(l_2) = Q^{Z_0,Z_{w2}^{\mp}} \cdot R^{Z_{w2}^{\mp},Z_{w2}^{\mp}} \cdot Q^{Z_{w2}^{\mp},Z_0} \tag{4}$$

where $Q^{Z_0,Z_{w1}^{\mp}}$ and $Q^{Z_0,Z_{w2}^{\mp}}$ are the WCMs for the impedance transformation from Z_0 to $Z_{w1}^{\mp}$ and from Z_0 to $Z_{w2}^{\mp}$, respectively; $R^{Z_{w1}^{\mp}}$ and $R^{Z_{w2}^{\mp}}$ denote the WCMs for the amplitude and phase variations throughout the reflection-asymmetric network and the reference network; $Q^{Z_{w1}^{\mp},Z_0}$ and $Q^{Z_{w2}^{\mp},Z_0}$ are the WCMs for the impedance transformation from $Z_{w1}^{\mp}$ to Z_0 and from $Z_{w2}^{\mp}$ to Z_0, respectively.

The WCMs $Q^{Z_0,Z_{w1}^{\mp}}$, $Q^{Z_0,Z_{w2}^{\mp}}$, $Q^{Z_{w1}^{\mp},Z_0}$, $Q^{Z_{w2}^{\mp},Z_0}$, $R^{Z_{w1}^{\mp},Z_{w1}^{\mp}}$, and $R^{Z_{w2}^{\mp},Z_{w2}^{\mp}}$ can be written [25] as

$$Q^{Z_0,Z_{w1}^{\mp}} = \kappa_1 \begin{bmatrix} 1 & \Gamma_{01}^{+} \\ \Gamma_{01}^{-} & 1 \end{bmatrix}, \tag{5}$$

$$Q^{Z_0,Z_{w2}^{\mp}} = \kappa_2 \begin{bmatrix} 1 & \Gamma_{02}^{+} \\ \Gamma_{02}^{-} & 1 \end{bmatrix}, \tag{6}$$

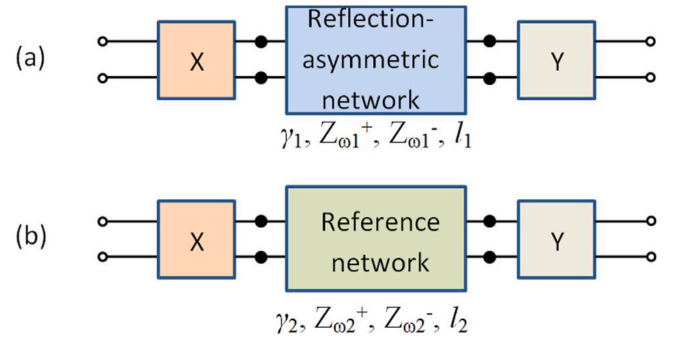

Fig. 1. Two configurations for the application of our method. (a) The configuration involving a reflection-asymmetric two-port network with forward and backward impedances Z_{w1}^{+} and Z_{w1}^{-}, the propagation constant γ_1, and the length l_1 between two two-port error networks X and Y and (b) the configuration involving a reference two-port network with known forward and backward impedances Z_{w2}^{+} and Z_{w2}^{-}, the propagation constant γ_2, and the length l_2 between the same two-port networks X and Y.

$$\Gamma_{01}^{+} = \frac{Z_{w1}^{+} - Z_0}{Z_{w1}^{+} + Z_0}, \quad \Gamma_{01}^{-} = \frac{Z_{w1}^{-} - Z_0}{Z_{w1}^{-} + Z_0}, \tag{7}$$

$$\Gamma_{02}^{+} = \frac{Z_{w2}^{+} - Z_0}{Z_{w2}^{+} + Z_0}, \quad \Gamma_{02}^{-} = \frac{Z_{w2}^{-} - Z_0}{Z_{w2}^{-} + Z_0}, \tag{8}$$

$$Q^{Z_{w1}^{\mp},Z_0} = \frac{1}{\kappa_1}\frac{1}{1-\Gamma_{01}^{+}\Gamma_{01}^{-}} \begin{bmatrix} 1 & -\Gamma_{01}^{+} \\ -\Gamma_{01}^{-} & 1 \end{bmatrix}, \tag{9}$$

$$Q^{Z_{w2}^{\mp},Z_0} = \frac{1}{\kappa_2}\frac{1}{1-\Gamma_{02}^{+}\Gamma_{02}^{-}} \begin{bmatrix} 1 & -\Gamma_{02}^{+} \\ -\Gamma_{02}^{-} & 1 \end{bmatrix}, \tag{10}$$

$$R^{Z_{w1}^{\mp},Z_{w1}^{\mp}} = \begin{bmatrix} T_1 & 0 \\ 0 & \frac{1}{T_1} \end{bmatrix}, \tag{11}$$

$$R^{Z_{w2}^{\mp},Z_{w2}^{\mp}} = \begin{bmatrix} T_2 & 0 \\ 0 & \frac{1}{T_2} \end{bmatrix}, \tag{12}$$

$$T_1 = e^{-\gamma_1 l_1}, \quad T_2 = e^{-\gamma_2 l_2}, \tag{13}$$

where κ_1 and κ_2 values can be evaluated by applying the electrical circuit theory [25,28]; Γ_{01}^{+}, Γ_{01}^{-}, Γ_{02}^{+}, and Γ_{02}^{-} are the interfacial reflection coefficients; and T_1 and T_2 are the propagation factors within the reflection-asymmetric network and the reference network, respectively.

Our goal is to eliminate the unknown networks X and Y from measurements M_1 and M_2. Toward this goal, we first perform the summation of M_1 and M_2, then take the determinants of $M_1 + M_2$ and M_2 (or M_1), and finally get the ratio of both determinant terms:

$$M_1 + M_2 = T_X \cdot \left[R_1^{Z_0,Z_0} + R_2^{Z_0,Z_0}\right] \cdot T_Y \tag{14}$$

$$\frac{\det(M_1+M_2)}{\det(M_2)} = \frac{\det(T_X)\cdot\det\left[R_1^{Z_0,Z_0}(l_1) + R_2^{Z_0,Z_0}(l_2)\right]\cdot\det(T_Y)}{\det(T_X)\cdot\det\left[R_1^{Z_0,Z_0}(l_2)\right]\cdot\det(T_Y)} \tag{15}$$

$$\frac{\det(M_1+M_2)}{\det(M_2)} = \frac{\det\left[\begin{array}{c} Q^{Z_0,Z_{w2}^{\mp}} \cdot Q^{Z_{w2}^{\mp},Z_{w1}^{\mp}} \cdot R_1^{Z_{w1}^{\mp},Z_{w1}^{\mp}}(l_1) \cdot Q^{Z_{w1}^{\mp},Z_{w2}^{\mp}} \\ \cdot Q^{Z_{w2}^{\mp},Z_0} + Q^{Z_0,Z_{w2}^{\mp}} \cdot R_2^{Z_{w2}^{\mp},Z_{w2}^{\mp}}(l_2) \cdot Q^{Z_{w2}^{\mp},Z_0} \end{array}\right]}{\det\left[Q^{Z_0,Z_{w2}^{\mp}} \cdot R_2^{Z_{w2}^{\mp},Z_{w2}^{\mp}}(l_2) \cdot Q^{Z_{w2}^{\mp},Z_0}\right]} \tag{16}$$

$$\frac{\det(M_1+M_2)}{\det(M_2)} = \frac{\det\left[Q^{Z_{w2}^{\mp},Z_{w1}^{\mp}} \cdot R_1^{Z_{w1}^{\mp},Z_{w1}^{\mp}}(l_1) \cdot Q^{Z_{w1}^{\mp},Z_{w2}^{\mp}} + R_2^{Z_{w2}^{\mp},Z_{w2}^{\mp}}(l_2)\right]}{\det\left[R_2^{Z_{w2}^{\mp},Z_{w2}^{\mp}}(l_2)\right]} \tag{17}$$

$$\frac{\det(M_1+M_2)}{\det(M_2)} = \det\left[Q^{Z_{w2}^{\mp},Z_{w1}^{\mp}} \cdot R_1^{Z_{w1}^{\mp},Z_{w1}^{\mp}}(l_1) \cdot Q^{Z_{w1}^{\mp},Z_{w2}^{\mp}} + R_2^{Z_{w2}^{\mp},Z_{w2}^{\mp}}(l_2)\right]. \quad (18)$$

It is noted that common terms in the numerator and the denominator in (14)–(18) are eliminated. Besides, it is seen from (18) that the expressions of $Q^{Z_{w2}^{\mp},Z_{w1}^{\mp}}$ and $Q^{Z_{w1}^{\mp},Z_{w2}^{\mp}}$ are needed to be known. Using the expressions of $Q^{Z_0,Z_{w1}^{\mp}}$, $Q^{Z_0,Z_{w2}^{\mp}}$, $Q^{Z_{w1}^{\mp},Z_0}$, and $Q^{Z_{w2}^{\mp},Z_0}$ in (5), (6), (9), and (10), it is possible to express $\det(M_1+M_2)/\det(M_2)$ in (18) as

$$\frac{\det(M_1+M_2)}{\det(M_2)} = \left[Q^{Z_{w2}^{\mp},Z_0} \cdot Q^{Z_0,Z_{w1}^{\mp}} \cdot R_1^{Z_{w1}^{\mp},Z_{w1}^{\mp}}(l_1) \cdot Q^{Z_{w1}^{\mp},Z_0} \cdot Q^{Z_0,Z_{w2}^{\mp}} + R_2^{Z_{w2}^{\mp},Z_{w2}^{\mp}}(l_2)\right]. \quad (19)$$

After incorporating the expressions in (5), (6), (12), and (13) into (19) and after some manipulations, we determine

$$\frac{\det(M_1+M_2)}{\det(M_2)} - 2 = \Omega_1 = \frac{T_1^2+T_2^2+(\Gamma_\Delta-1)\left(1+T_1^2T_2^2\right)}{\Gamma_\Delta T_1 T_2} \quad (20)$$

where

$$\Gamma_\Delta = \frac{(1-\Gamma_{01}^{+}\Gamma_{01}^{-})(1-\Gamma_{02}^{+}\Gamma_{02}^{-})}{(1-\Gamma_{01}^{+}\Gamma_{02}^{-})(1-\Gamma_{01}^{-}\Gamma_{02}^{+})}. \quad (21)$$

2.1. Zero-length line reference network (thru connection)

It is seen from (20) that the zero-length reference network ($l_2 = 0$) reduces it to the following simple relation [25]:

$$\Omega_1 = T_1 + 1/T_1, \quad (22)$$

from which one can easily determine T_1 by enforcing the passivity condition ($|T_1| \le 1$ where $|\star|$ denotes the magnitude of '$\star$') without knowing any information about Γ_{01}^{+} and Γ_{01}^{-}.

Then, the propagation constant γ_1 of the reflection-asymmetric network can be evaluated from

$$\gamma_1 = \frac{-\ln(T_1) \mp j2\pi m_b}{l_1}, \quad m_b = 0,1,2,\ldots \quad (23)$$

where m_b denotes the branch index term whose value can be determined by using the stepwise method [29] or the phase unwrapping method [30].

2.2. Nonzero-length reference network

It is obvious from (20) and (21) that an additional measurement is needed to extract T_1 if $l_2 \neq 0$. Assuming that there is another reference network having the same forward and backward wave impedances $Z_{w3}^{+} = Z_{w2}^{+}$ and $Z_{w3}^{-} = Z_{w2}^{-}$, and propagation constant γ_2, but a different length l_3 ($l_3 \neq l_2$), then it is possible to derive T_1 from the following quadratic equation

$$T_1^2 + \chi T_1 + 1 = 0, \quad (24)$$

where

$$\chi = \frac{\Omega_1(1-T_3^2)T_2 - \Omega_2(1-T_2^2)T_3}{T_3^2 - T_2^2}, \quad T_3 = e^{-\gamma_2 l_3}, \quad (25)$$

$$\frac{\det(M_1+M_3)}{\det(M_3)} - 2 = \Omega_2 = \frac{T_1^2+T_3^2+(\Gamma_\Delta-1)\left(1+T_1^2T_3^2\right)}{\Gamma_\Delta T_1 T_3}, \quad (26)$$

from which one can determine T_1 as

$$T_1 = \frac{-\chi \mp \sqrt{\chi^2-4}}{2}. \quad (27)$$

The correct solution for T_1 from (27) can be ascertained by enforcing the passivity condition, as discussed above.

Finally, the propagation constant γ_1 of the reflection-asymmetric network can be determined from (23).

3. Measurement and discussion

A measurement setup, as shown in Fig. 2(a), constructed by a rectangular waveguide apparatus operating at X-band (8.2–12.4 GHz) was utilized to validate the proposed method [25]. A handheld VNA (N9918 A) purchased from the company Keysight Technologies was operated as a source for electromagnetic signals and a measuring instrument for S-parameters. Two highly-precise coaxial lines (1 m in length) were employed between the VNA ports and two coaxial-to-waveguide adapters to transfer signals from the VNA. Two additional longer waveguide sections with lengths greater than at least two free-space wavelengths at 8.2 GHz were in change for eliminating higher order modes which can appear in the measurement cell. S-parameter measurements were carried out for 1001 points at X-band.

For validation of our method, as for the reflection-asymmetric network, we considered an X-band rectangular waveguide loaded with a bianisotropic MM slab with length l_1 = 10.16 mm [25]. This MM slab was constructed by SRRs whose geometry and coordinate axes are shown in Fig. 2(b). It has a metallization length L_m = 2.00 mm, width w = 0.30 mm, and gap g = 0.30 mm. Metallic tracks of SRRs were manufactured by copper with conductivity $\sigma_c = 5.8\times10^7$ S/m and thickness t_m = 35 μm. The substrate has thickness d = 1.5 mm, length l_1 = 10.16 mm, dielectric constant ε_d = 4.3, and loss tangent δ_e = 0.025. The whole MM slab is repeated 7 times in the x axis and 4 times in the y axis after SRR was sandwiched between two substrates, as shown in Fig. 2(c). The slab has the periodicity u_x = 3.035 mm and u_y = 2.54 mm in the x and y directions, both of which are greater than the free-space wavelength (30 mm) at f = 10 GHz. Further details about the construction of this slab and its fabrication are presented in the study [25].

Fig. 2(d) illustrates the frequency dependence of magnitudes of measured S_{11}, S_{21} ($\approx S_{12}$), and S_{22} (dashed lines) of this slab, after the measurement setup was calibrated by the thru-reflect-line (TRL) calibration technique [31]. For the line and reflect standards, a 9.40 mm waveguide washer and a highly reflective short termination were employed, respectively. It is seen from Fig. 2(d) that the bianisotropic MM slab has a resonance near 11.5 GHz and has asymmetric reflection property over full frequency band due to coupling between electric and magnetic resonances [32]. To validate measured S-parameters, S-parameters of the designed MM slab are simulated by using a full 3D electromagnetic simulation program (CST Microwave Studio). Perfect electric conductors (E_t = 0) were considered as boundaries of the waveguide and waveguide ports were located in the z-axis at appropriate planes to input electromagnetic energy and extract S-parameters. For more information about simulation details, the reader can refer to the study [25]. It is noted from Fig. 2(d) that simulated (solid lines) and measured S-parameters are in good agreement over the whole frequency band.

To extract propagation constant of the designed MM slab by our proposed formalism, two different types of reference networks were utilized. For the first reference network, two empty waveguide straights with lengths l_2 = 7.70 mm and l_3 = 9.40 mm were considered. Besides, for the second reference network, these empty waveguide straights were fully filled with two PE samples with lengths equal to the lengths of their corresponding waveguide straights (l_2 = 7.70 mm and l_3 = 9.40 mm). Figs. 3 and 4 show extracted real and imaginary parts of T_1 and γ_1 by the proposed method for these two cases using average values of uncalibrated S-parameters from ten linearly-independent measurements, after applying the rolling average method [18]. To validate our method, T_1 and γ_1 were also retrieved by the calibration-dependent method [27] using measured calibrated S-parameters in Fig. 2(d) and by the calibration-independent thru-line method [25] using non-calibrated S-parameters. It should be stressed here that in implementation of the method in [25], the expression of T_1 in (22) was applied.

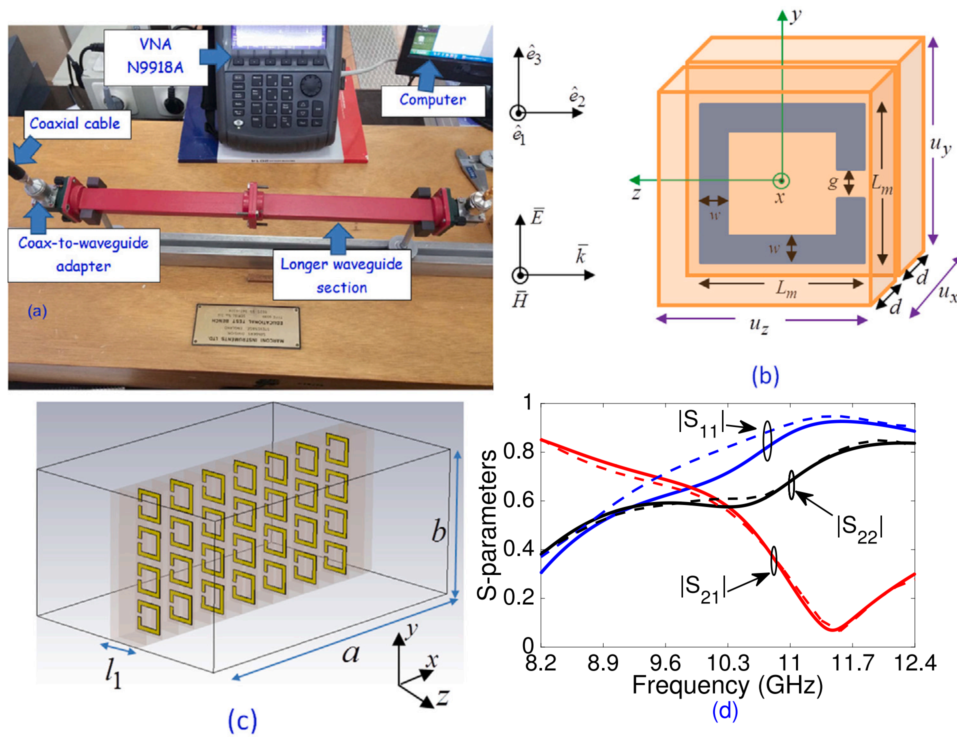

Fig. 2. (a) A photo of the measurement setup, (b) geometry of the bianisotropic MM unit cell in addition to coordinate axis, (c) constructed MM slab after repetition of the MM cell in (b) 7 times and 4 times in the x- and the y-axes, and (d) magnitudes of simulated (solid lines) and measured (dashed lines) S-parameters of this slab within rectangular waveguide (IEEE © [27]).

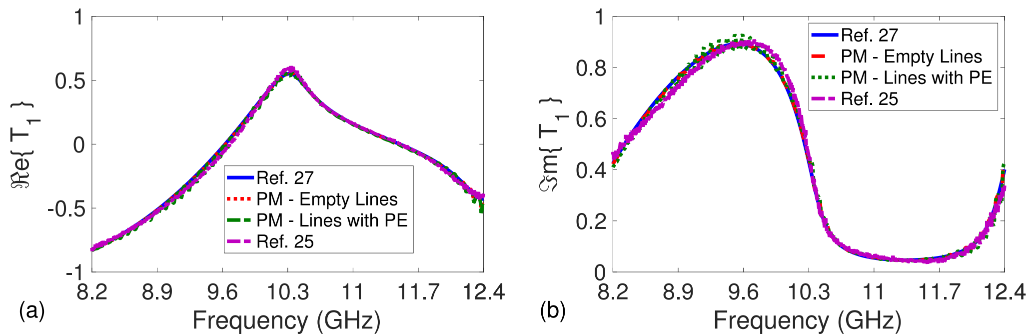

Fig. 3. (a) Real and (b) imaginary parts of T_1 retrieved by the calibration-dependent method [27] (shown by solid lines and denoted by 'Ref. 27'), by the calibration-independent thru-line method [25] (shown by dashdot lines and denoted by 'Ref. 25'), and the proposed method for two cases: (i) two empty X-band lines with l_2 = 7.70 and l_3 = 9.40 mm (shown by dashed lines and denoted by 'PM - Empty Lines') and (ii) the same lines loaded fully with PE samples (shown by dotted lines and denoted by 'PM - Lines with PE').

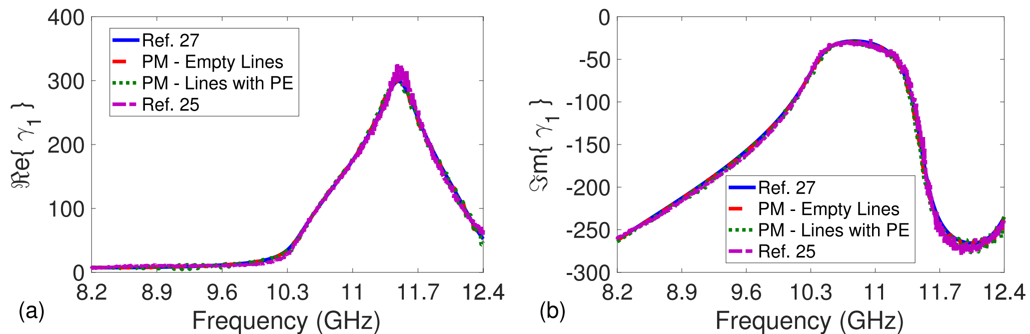

Fig. 4. (a) Real and (b) imaginary parts of γ_1 retrieved by the calibration-dependent method [27] (shown by solid lines and denoted by 'Ref. 27'), by the calibration-independent thru-line method [25] (shown by dashdot lines and denoted by 'Ref. 25'), and the proposed method for two cases: (i) two empty X-band lines with l_2 = 7.70 and l_3 = 9.40 mm (shown by dashed lines and denoted by 'PM - Empty Lines') and (ii) the same lines loaded fully with PE samples (shown by dotted lines and denoted by 'PM - Lines with PE').

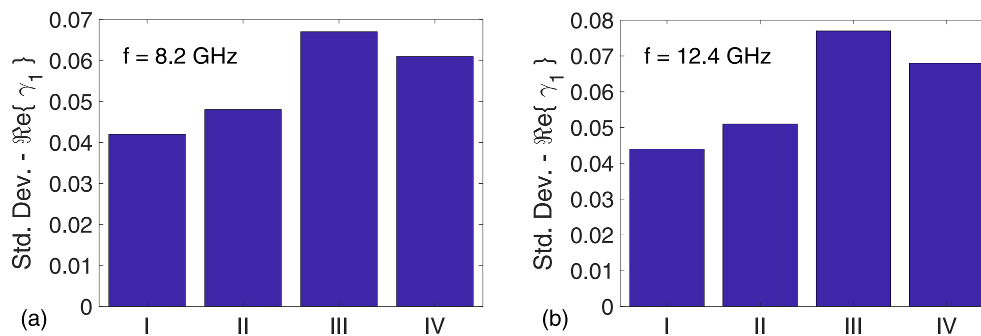

Fig. 5. Calculated standard deviations at (a) $f = 8.2$ GHz and (b) $f = 12.4$ GHz for γ_1 extracted by different methodologies (i) the calibration-dependent method [27] (denoted by 'I'), (ii) the proposed method using two empty X-band lines with $l_2 = 7.70$ and $l_3 = 9.40$ mm (denoted by 'II'), (iii) the proposed method using two X-band lines with $l_2 = 7.70$ and $l_3 = 9.40$ mm loaded fully with PE samples (denoted by 'III'), and (iv) the calibration-independent thru-line method [25] (denoted by 'IV').

The following points are noted from results in Figs. 3 and 4. First, real and imaginary parts of T_1 (and γ_1) retrieved by our method for both cases (both reference networks) are in good agreement with those extracted by the calibration-dependent method [27] and by the calibration-independent thru-line method [25]. This obviously validates our formalism for empty and PE-loaded reference networks. Second, extracted real and imaginary parts of T_1 (and γ_1) by our method for the second reference network have slightly greater ripples than those for the first reference network, which we think is due to sample irregularities or inhomogeneities [33]. To examine this point further and compare the performance of our method with those in the studies [25, 27], standard deviations obtained from ten independent measurements for $\Re e\{\gamma_1\}$ extracted by our method and the methods in the studies [25,27] are presented at two discrete frequencies ($f = 8.2$ GHz and 12.4 GHz), as shown in Figs. 5(a) and 5(b), respectively. It is observed from Figs. 5(a) and 5(b) that standard deviations for $\Re e\{\gamma_1\}$ determined from the calibration-dependent method [27] and the proposed method using the reference network composed of empty waveguide sections are greatly lower than those determined from the calibration-independent method [25] and the proposed method using the reference network composed of waveguide sections loaded by PE samples. It should be mentioned here that although the standard deviation for $\Re e\{\gamma_1\}$ determined from the proposed method using the reference network composed of empty waveguide sections is slightly greater than that determined from the calibration-dependent method [27], this method necessitates a prior calibration technique before extraction process while our proposed formalism does not require any formal calibration procedure. Third, our proposed formalism is more flexible than the method in the study [25], because it allows non-calibrated measurements of zero-length (thru) or non-zero length transmission lines with arbitrary propagation constant and wave impedances. Thanks to this flexibility, the accuracy of our proposed method could be improved in extraction of propagation constant of networks with asymmetric reflections.

4. Conclusion

A new formalism based on the line–line methodology is proposed to improve the accuracy and give additional flexibility in γ_1 measurement of networks with asymmetric reflections using non-calibrated S-parameter measurements. It considers a reference network with arbitrary forward and backward wave impedances, propagation constant, and length for such extraction, thereby giving flexibility in the application of the line–line methods for γ_1 measurement of reflection-asymmetric networks. Our proposed method was validated by γ_1 measurement of a reflection-asymmetric network (waveguide) constructed by a bianisotropic MM slab composed of C-shaped SRRs. Two different kinds of reference networks were utilized for T_1 and γ_1 measurements of this reflection-asymmetric network using average values of ten independent S-parameter measurements (and the standard deviation of $\Re e\{\gamma_1\}$) and thus performance evaluation of our method. While the first kind was composed of two empty waveguide sections with different lengths ($l_2 = 7.70$ mm and $l_3 = 9.40$ mm), the second kind was composed of the same waveguide sections fully loaded by PE samples. The following main results are observed from T_1, γ_1, and $\Re e\{\gamma_1\}$ measurements. First, real and imaginary parts of T_1 and γ_1 extracted by our method for both kinds of reference networks are in good agreement with those extracted by the tested calibration-independent method and the tested another calibration-independent method. Second, standard deviations for $\Re e\{\gamma_1\}$ evaluated by our method using the second kind of reference network at the lowest frequency ($f = 8.2$ GHz) and the highest frequency ($f = 12.4$ GHz) are, respectively, close to those evaluated from the tested calibration-independent method and are significantly smaller than those evaluated from the tested calibration-independent method and those evaluated from our method using the first kind of reference network. Therefore, the accuracy of our proposed method could be improved by selecting suitable reference networks.

CRediT authorship contribution statement

Ugur Cem Hasar: Conceptualization, Methodology, Investigation, Writing – original draft. **Hamdullah Ozturk:** Visualization, Writing – review & editing. **Huseyin Korkmaz:** Visualization, Writing – review & editing. **Mucahit Izginli:** Visualization, Writing – review & editing. **Muharrem Karaaslan:** Investigation, Writing – review & editing.

Declaration of competing interest

The authors declare that they have no known competing financial interests or personal relationships that could have appeared to influence the work reported in this paper.

Acknowledgments

Authors would like to thank the Scientific and Technological Research Council of Turkey (TUBITAK) under grant number 120M763 for providing the support to conduct our research. H. Ozturk and H. Korkmaz also acknowledge the TUBITAK BIDEB 2211/C program for supporting their studies.

References

[1] K.H. Baek, H.Y. Sung, W.S. Park, A 3-position transmission/reflection method for measuring the permittivity of low loss materials, IEEE Microw. Guid. Wave Lett. 5 (1) (1995) 3–5.

[2] M.Q. Lee, S. Nam, An accurate broadband measurement of substrate dielectric constant, IEEE Microw. Guid. Wave Lett. 6 (4) (1996) 168–170.

[3] C. Wan, B. Nauwelaers, W.D. Raedt, M.V. Rossum, Complex permittivity measurement method based on asymmetry of reciprocal two-ports, Electron. Lett. 32 (16) (1996) 1497.
[4] C. Wan, B. Nauwelaers, W.D. Raedt, M.V. Rossum, Two new measurement methods for explicit determination of complex permittivity, IEEE Trans. Microw. Theory Tech. 46 (11) (1998) 1614–1619.
[5] M.D. Janezic, J.A. Jargon, Complex permittivity determination from propagation constant measurements, IEEE Microw. Guid. Wave Lett. 9 (2) (1999) 76–78.
[6] J.A. Reynoso-Hernandez, C.F. Estrada-Maldonado, T. Parra, K. Grenier, J. Graffeuil, An improved method for estimation of the wave propagation constant in broadband uniform millimeter wave transmission line, Microw. Opt. Technol. Lett. 22 (4) (1999) 268–271.
[7] I. Huygen, C. Steukers, F. Duhamel, A wideband line-line dielectrometric method for liquids, soils, and planar substrates, IEEE Trans. Instrum. Meas. 50 (5) (2001) 1343–1348.
[8] L. Lanzi, M. Carla, C.M.C. Gambi, L. Lanzi, Differential and double-differential dielectric spectroscopy to measure complex permittivity in transmission lines, Rev. Sci. Instrum. 73 (8) (2002) 3085–3088.
[9] J.A. Reynoso-Hernandez, Unified method for determining the complex propagation constant of reflecting and nonreflecting transmission lines, IEEE Microw. Wirel. Compon. Lett. 13 (8) (2003) 351–353.
[10] U.C. Hasar, A new calibration-independent method for complex permittivity extraction of solid dielectric materials, IEEE Microw. Wirel. Compon. Lett. 18 (12) (2008) 788–790.
[11] U.C. Hasar, A calibration-independent method for accurate complex permittivity determination of liquid materials, Rev. Sci. Instrum. 79 (8) (2008).
[12] U.C. Hasar, Calibration-independent method for complex permittivity determination of liquid and granular materials, Electron. Lett. 44 (9) (2008).
[13] K. Grenier, D. Dubuc, P. Poleni, M. Kumemura, H. Toshiyoshi, T. Fujii, H. Fujita, Integrated broadband microwave and microfluidic sensor dedicated to bioengineering, IEEE Trans. Microw. Theory Tech. 57 (12) (2009) 3246–3253.
[14] U.C. Hasar, O. Simsek, A calibration-independent microwave method for position-insensitive and nonsingular dielectric measurements of solid materials, J. Phys. D: Appl. Phys. 42 (7) (2009).
[15] U.C. Hasar, O.E. Inan, A position-invariant calibration-independent method for permittivity measurement, Microw. Opt. Technol. Lett. 51 (6) (2009).
[16] N.J. Farcich, J. Salonen, P.M. Asbeck, Single-length method used to determine the dielectric constant of polydimethylsiloxane, IEEE Trans. Microw. Theory Tech. 56 (12) (2008) 2963–2971.
[17] Z. Caijun, J. Quanxing, J. Shenhui, Calibration-independent and position-insensitive transmission/reflection method for permittivity measurement with one sample in coaxial line, IEEE Trans. Electromagn. Compat. 53 (3) (2011) 684–689.
[18] N. Jebbor, S. Bri, A.M. Sànchez, M. Chaibi, A fast calibration-independent method for complex permittivity determination at microwave frequencies, Measurement 46 (7) (2013) 2206–2209.
[19] C. Guoxin, Calibration-independent measurement of complex permittivity of liquids using a coaxial transmission line, Rev. Sci. Instrum. 86 (1) (2015) 014704.
[20] U.C. Hasar, Explicit permittivity determination of medium-loss materials from calibration-independent measurements, IEEE Sens. J. 16 (13) (2016) 5177–5182.
[21] U.C. Hasar, Thickness-invariant complex permittivity retrieval from calibration-independent measurements, IEEE Microw. Wirel. Compon. Lett. 27 (2) (2017) 201–203.
[22] U.C. Hasar, Self-calibrating transmission–reflection technique for constitutive parameters retrieval of materials, IEEE Trans. Microw. Theory Tech. 66 (2) (2018) 1081–1089.
[23] J.E. Zuniga-Juarez, J.A. Reynoso-Hernandez, J.R. Loo-Yau, M.C. Maya-Sanchez, An improved two-tier L-L method for characterizing symmetrical microwave test fixtures, Measurement 44 (9) (2011) 1491–1498.
[24] L. Tong, Haihui Zha, Xingfa Gu, The complex permittivity measurement of powder materials and the dielectric constant of lunar soil, Measurement 48 (2014) 6–12.
[25] U.C. Hasar, Propagation constant measurement of microwave networks with symmetric/asymmetric reflections, IEEE Sens. J. 18 (12) (2018) 4940–4946.
[26] F. Razzaz, M. Alkanhal, Electromagnetic tunneling and resonances in pseudochiral omega slabs, Sci. Rep. 7 (2017) 41961.
[27] U.C. Hasar, A. Muratoglu, M. Bute, J.J. Barroso, M. Ertugrul, Effective constitutive parameters retrieval method for bianisotropic metamaterials using waveguide measurements, IEEE Trans. Microw. Theory Tech. 65 (5) (2017) 1488–1497.
[28] R.B. Marks, D.F. Williams, A general waveguide circuit theory, J. Res. Natl. Inst. Stand. Technol. 97 (5) (1992) 533–562.
[29] U.C. Hasar, J.J. Barroso, C. Sabah, Y. Kaya, M. Ertugrul, Stepwise technique for accurate and unique retrieval of electromagnetic properties of bianisotropic metamaterials, J. Opt. Soc. Amer. B 30 (4) (2013) 1058–1068.
[30] J.J. Barroso, U.C. Hasar, Constitutive parameters of a metamaterial slab retrieved by the phase unwrapping method, J. Infrared Millim. Terahz Waves 33 (2012) 237–244.
[31] G.F. Engen, C.A. Hoer, Thru-reflect-line: An improved technique for calibrationg the dual 6-port automatic network analyzer, IEEE Trans. Microw. Theory Tech. 27 (12) (1979) 983–987.
[32] G. Ozturk, U.C. Hasar, M. Bute, M. Ertugrul, Determination of constitutive parameters of strong-coupled bianisotropic metamaterials using oblique incidence scattering parameters, IEEE Trans. Antennas and Propagation 69 (2) (2021) 918–927.
[33] U.C. Hasar, Y. Kaya, G. Ozturk, M. Ertugrul, Effect of sample deformation in longitudinal axis on material parameter extraction by waveguides, Measurement 176 (2021) 109175.